Phase diagrams and physical properties of single-domain epitaxial $Pb(Zr_{1-x}Ti_x)O_3$ thin films

N. A. Pertsev,* V. G. Kukhar, H. Kohlstedt, and R. Waser

Institut für Festkörperforschung, Forschungszentrum Jülich, D-52425 Jülich, Germany

The equilibrium polarization states and physical properties of single-domain $Pb(Zr_{1-x}Ti_x)O_3$ (PZT) thin films epitaxially grown on dissimilar cubic substrates have been examined by a nonlinear thermodynamic theory. In contrast to the former theoretical studies of PZT films, the two-dimensional straining and clamping of a film by a thick substrate is correctly taken into account in the reported calculations. The "misfit strain-temperature" phase diagrams are developed for PZT films of several different compositions ($x = 0.9$, 0.8, 0.7, 0.6, 0.5, and 0.4). The characteristic feature of these diagrams is the presence of a "monoclinic gap" separating the stability ranges of the tetragonal out-of-plane and the orthorhombic in-plane polarization states. It is found that this gap widens with the increase of Zr content, and its center shifts from positive values of the misfit strain towards zero. The dependences of the polarization components on the misfit strain and composition at the room temperature are calculated and compared with the available experimental data. The small-signal dielectric and piezoelectric responses of single-domain PZT films are also determined, and their misfit-strain dependence is discussed.

I. INTRODUCTION

Ferroelectric $Pb(Zr_{1-x}Ti_x)O_3$ (PZT) solid solutions are currently attracting great interest for both practical and fundamental reasons. On the one hand, PZT ceramics and thin films have a wide range of implemented and potential device applications.[1–3] On the other hand, an unusual (morphotropic) boundary exists in the phase diagram of bulk PZT, near which this ferroelectric material exhibits anomalous piezoelectric and dielectric properties.[4] The morphotropic phase boundary (MPB) is situated around $x = 0.45–0.50$ in the composition-temperature plane, and separates the stability range of the tetragonal ground state from that of the rhombohedral one. The recent discovery by Noheda and co-workers[5,6] of an intermediate monoclinic phase in the PZT ceramic with a composition close to the MPB ($x = 0.48$) demonstrates that PZT solid solutions still represent an object of high fundamental interest.

For bulk PZT, the physical and structural properties were investigated theoretically in many papers. Important results were obtained by Haun *et al.*[7] with the aid of a Landau-Ginsburg-Devonshire-type phenomenological theory. Using an expansion of the free energy up to the sixth order in the polar order parameter, these authors were able to explain the observed phase states and physical properties of PZT ceramics over the entire range of compositions. Though the developed sixth-order theory cannot support a monoclinic phase, an extension of the thermodynamic calculations to the eighth order makes it possible to describe the newly discovered monoclinic phase in a natural way.[8] The existence of a low-temperature monoclinic phase is also confirmed by the simulations based on a first-principles effective Hamiltonian approach.[9] Moreover, these theoretical calculations provide an explanation for the high piezoelectric response of PZT ceramics near the MPB.[9]

Thin films of PZT require a separate theoretical analysis since the properties of ferroelectric films often differ markedly from those of bulk ferroelectrics. Oh and Jang[10] suggested that the MPB in epitaxial PZT films may be shifted towards a higher Zr content due to internal mechanical stresses existing in thin films grown on a dissimilar thick substrate. They attempted to describe the mechanical substrate effect via the introduction of a biaxial in-plane stress into the thermodynamic theory of bulk PZT developed by Haun *et al.*[7] This stress was assumed to be independent of the polarization state of a ferroelectric film and regarded as a constant parameter during the minimization of the film free energy. However, it is known that this simple assumption does not hold for epitaxial thin films.[11] In reality, the in-plane lattice *strains* appear to be fixed parameters of the film at a given temperature,[11] so that the associated biaxial *stress* is a function of the orientation and magnitude of the polarization vector in the epitaxial layer (see Sec. II). Therefore, the influence of mechanical film/substrate interaction on the ferroelectricity in PZT films still requires a rigorous theoretical description similar to that developed in Refs. 11–14 for $BaTiO_3$, $PbTiO_3$, and $SrTiO_3$ epitaxial thin films. The correct solution of this problem is especially desirable in view of the successful fabrication of epitaxial PZT films on various substrates in many laboratories worldwide.[15–24] Remarkably, the single-crystal PZT films covering the full compositional range have been already prepared and characterized.[19]

In this paper, we report the thermodynamic calculations of the polarization states and physical properties of single-crystalline PZT films, which correctly take into account the actual stress-strain conditions existing in an epitaxial overlayer. Thin films are supposed to be grown in a paraelectric phase on thick (001)-oriented cubic substrates. In accordance with the experimental results,[19] we assume that a cube-on-cube epitaxial relationship is established between the growing film and the substrate for all compositions. In this situation, the mechanical substrate effect on the film properties is

governed by a scalar parameter, i.e., by the *misfit strain* S_m in the epitaxial system (see Sec. II). The misfit strain plays the role of an external parameter in our thermodynamic theory instead of biaxial internal stress used in Ref. 10. Accordingly, the equilibrium polarization state of a (short-circuited) epitaxial PZT film is predicted to depend on the misfit strain S_m, temperature T, and Ti content x. The stability ranges of various possible polarization states may be conveniently described with the aid of the "misfit strain-temperature" phase diagrams[11] computed for PZT films of different compositions.

Our calculations are based on the sixth-order thermodynamic theory developed for bulk PZT by Haun *et al.*[7] The introduction of the eighth-order polarization terms into this theory is not possible at present, because numerical values of the corresponding coefficients are not known. However, since the free-energy expansion up to sixth order is sufficient for the prediction of stable polarization states with a monoclinic symmetry in strained ferroelectric films,[11,14] the eighth-order terms, which are necessary to describe the newly discovered monoclinic phase in bulk PZT,[8] may be ignored in the first approximation. (The eighth-order terms will only change positions of the boundaries of a monoclinic gap on the misfit strain-temperature phase diagram. We believe that these changes will be small because the sixth-order theory[7] does not explain the properties of bulk PZT only in a very narrow range of compositions near the MPB, where the monoclinic phase appears.) We also neglect the degrees of freedom associated with the tilting of the oxygen octahedra and the antiferroelectric-type polarization, which manifest themselves in the phase diagram of bulk PZT only at Zr contents larger than 0.6 (at $T \geq 25\,°C$).[4,7] To ensure a good accuracy of this approximation, we restrict our thermodynamic calculations by compositions $x \geq 0.4$ and temperatures above $T = 0\,°C$.

In Sec. II, the thermodynamics of single-domain epitaxial ferroelectric films is briefly discussed. The formation of ferroelastic domains (twins), which may occur in strained PZT films,[19,21] is not taken into account on the present stage of calculations. (Nonlinear thermodynamic description of polydomain states in PZT films is in progress and will be reported in a separate paper.) The misfit strain-temperature phase diagrams calculated for short-circuited single-domain PZT films with compositions $x = 0.9$, 0.8, 0.7, 0.6, 0.5, and 0.4 are reported in Sec. III. Section IV describes the dielectric and piezoelectric properties of single-domain PZT films. Finally, we discuss the most important theoretical predictions and compare them with the experimental data available for PZT thin films (Sec. V).

II. THERMODYNAMICS OF SINGLE-DOMAIN PZT FILMS

As shown in Ref. 11, the standard elastic Gibbs energy function G, which is employed in the thermodynamic theory of bulk ferroelectric crystals,[7,25] cannot be used to determine the equilibrium polarization states in epitaxial thin films. Indeed, the minima of G correspond to the stable thermodynamic states at fixed mechanical *stresses*.[25] In a thin film

grown on a much thicker substrate, however, the in-plane lattice *strains* remain constant due to the mechanical film/substrate interaction, whereas the related stresses are variable quantities depending on the film polarization state.[11] Evidently, the elastic energy associated with these internal stresses should give a *positive* contribution to the total free energy of a thin film. The elastic-energy term in the Gibbs function G, on the contrary, is itself negative.[25] Therefore, the calculations of Oh and Jang,[10] which were performed for PZT films using the function G, in fact lead to a physically unacceptable result, predicting that an increase in the biaxial in-plane stress reduces the film energy via the elastic contribution.

For single-domain ferroelectric films, the energetically most favorable polarization states can be found by minimizing the modified thermodynamic potential $\tilde{G}$ introduced in Ref. 11. This potential is defined by the relation $\tilde{G} = G + S_1\sigma_1 + S_2\sigma_2 + S_6\sigma_6$, where σ_n and S_n ($n = 1,2,3,...6$) are the stresses and strains in the Voigt matrix notation, and we use the rectangular reference frame (x_1, x_2, x_3) with the x_3 axis perpendicular to the film/substrate interface. In the case of (001)-oriented perovskite-type films grown on cubic substrates with the surface parallel to the (001) crystallographic plane, the boundary conditions give $S_1 = S_2 = S_m$ and $S_6 = 0$ for the lattice strains in the film plane.[11] Here $S_m = (b* - a_0)/a_0$ is the misfit strain in an epitaxial system, which is defined by the substrate effective lattice parameter[26] $b*$ and the equivalent cubic cell constant a_0 of the free standing film. If there are no tractions acting on the free surface of the film, we also have $\sigma_3 = \sigma_4 = \sigma_5 = 0$ owing to the boundary conditions. The remaining three internal stresses (σ_1, σ_2, and σ_6) and three lattice strains (S_3, S_4, and S_5) depend on the polarization **P** in the film. They can be calculated using the relationships $S_n = -\partial G/\partial \sigma_n$, which describe the elastic equation of state of a ferroelectric crystal.[7] The calculation gives

$$\sigma_1 = \frac{S_m}{s_{11}+s_{12}} - \frac{(s_{11}Q_{11}-s_{12}Q_{12})P_1^2 + (s_{11}Q_{12}-s_{12}Q_{11})P_2^2}{s_{11}^2 - s_{12}^2}$$
$$- \frac{Q_{12}}{s_{11}+s_{12}}P_3^2, \tag{1}$$

$$\sigma_2 = \frac{S_m}{s_{11}+s_{12}} - \frac{(s_{11}Q_{12}-s_{12}Q_{11})P_1^2 + (s_{11}Q_{11}-s_{12}Q_{12})P_2^2}{s_{11}^2 - s_{12}^2}$$
$$- \frac{Q_{12}}{s_{11}+s_{12}}P_3^2, \tag{2}$$

$$\sigma_6 = -\frac{Q_{44}}{s_{44}}P_1 P_2, \tag{3}$$

$$S_3 = \frac{2s_{12}}{s_{11}+s_{12}}S_m + \left[Q_{12} - \frac{s_{12}(Q_{11}+Q_{12})}{s_{11}+s_{12}}\right](P_1^2+P_2^2)$$
$$+ \left(Q_{11} - \frac{2s_{12}Q_{12}}{s_{11}+s_{12}}\right)P_3^2, \tag{4}$$

$$S_4 = Q_{44} P_2 P_3, \qquad (5)$$

$$S_5 = Q_{44} P_1 P_3, \qquad (6)$$

where P_i ($i=1,2,3$) are the polarization components in the crystallographic reference frame of the paraelectric phase, s_{ln} are the elastic compliances at constant polarization, and Q_{ln} are the electrostrictive constants in polarization notation. Equations (1)–(3) show that the assumption of Oh and Jang,[10] who regarded the stresses σ_1, σ_2, and σ_6 as constant external parameters, does not hold for epitaxial ferroelectric films. Moreover, in the polarization states with $P_1 \neq 0$ and $P_2 \neq 0$, the shear stress σ_6 differs from zero, which was not taken into account in Ref. 10.

The substitution of Eqs. (1)–(3) into the general expression for the modified thermodynamic potential $\tilde{G}$ makes it possible to present $\tilde{G}$ in the convenient form[11]

$$\tilde{G} = \frac{S_m^2}{s_{11}+s_{12}} + a_1^*(P_1^2+P_2^2) + a_3^* P_3^2 + a_{11}^*(P_1^4+P_2^4)$$
$$+ a_{12}^* P_1^2 P_2^2 + a_{13}^*(P_1^2+P_2^2)P_3^2 + a_{33}^* P_3^4$$
$$+ a_{111}(P_1^6+P_2^6+P_3^6) + a_{112}[P_1^4(P_2^2+P_3^2)$$
$$+ P_2^4(P_1^2+P_3^2) + P_3^4(P_1^2+P_2^2)] + a_{123}P_1^2 P_2^2 P_3^2$$
$$- P_1 E_1 - P_2 E_2 - P_3 E_3, \qquad (7)$$

where

$$a_1^* = a_1 - S_m \frac{Q_{11}+Q_{12}}{s_{11}+s_{12}}, \qquad (8)$$

$$a_3^* = a_1 - S_m \frac{2Q_{12}}{s_{11}+s_{12}}, \qquad (9)$$

$$a_{11}^* = a_{11} + \frac{1}{2} \frac{1}{s_{11}^2 - s_{12}^2} [(Q_{11}^2+Q_{12}^2)s_{11} - 2Q_{11}Q_{12}s_{12}], \qquad (10)$$

$$a_{33}^* = a_{11} + \frac{Q_{12}^2}{s_{11}+s_{12}}, \qquad (11)$$

$$a_{12}^* = a_{12} - \frac{1}{s_{11}^2 - s_{12}^2}[(Q_{11}^2+Q_{12}^2)s_{12} - 2Q_{11}Q_{12}s_{11}] + \frac{Q_{44}^2}{2s_{44}}, \qquad (12)$$

$$a_{13}^* = a_{12} + \frac{Q_{12}(Q_{11}+Q_{12})}{s_{11}+s_{12}}, \qquad (13)$$

a_1, a_{ij}, and a_{ijk} are the dielectric stiffness and higher-order stiffness coefficients at constant stress, and E_i ($i=1,2,3$) are the components of an electric field **E** in the film, which is assumed to be uniform. Using Eq. (7), which defines $\tilde{G}$ as a function of the polarization components P_1, P_2, and P_3 in an epitaxial layer, it is possible to find all minima of the film thermodynamic potential $\tilde{G}(\mathbf{P})$. The comparison of these minima then enables the determination of the energetically

TABLE I. Elastic compliances s_{ln} of the paraelectric phase (in units of 10^{-12} Pa^{-1}) used in the thermodynamic calculations performed for PZT solid solutions.

Ti content x	0.9	0.8	0.7	0.6	0.5	0.4
s_{11}	8.1	8.2	8.4	8.6	10.5	8.8
s_{12}	−2.5	−2.6	−2.7	−2.8	−3.7	−2.9
s_{44}	12	14.4	17.5	21.2	28.7	24.6

most favorable polarization state of a single-domain film. Since the renormalized dielectric stiffnesses a_1^* and a_3^* are linear functions of the misfit strain S_m [see Eqs. (8) and (9)], the magnitude and spatial orientation of the polarization vector **P** in the equilibrium thermodynamic state should vary with the misfit strain in the film/substrate system. The temperature dependence of ferroelectricity in PZT films is mainly governed by that of the dielectric stiffness $a_1 = (T - \theta)/2\varepsilon_0 C$ since the higher-order stiffness coefficients a_{ij} and a_{ijk} may be taken as temperature-independent parameters (θ and C are the Curie-Weiss temperature and constant, and ε_0 is the permittivity of the vacuum).[7]

The above minimization procedure opens a way for the detailed theoretical description of single-domain polarization states, which may form in PZT films grown on dissimilar substrates. In the absence of electric field in an epitaxial layer (**E**=0), the stability ranges of the equilibrium states may be defined with the aid of the misfit strain-temperature phase diagrams developed in the next section. Using these diagrams, the small-signal dielectric and piezoelectric responses of PZT films can be calculated from Eqs. (7)–(13) as functions of the misfit strain and temperature (see Sec. IV).

III. PHASE DIAGRAMS OF SINGLE-DOMAIN PZT FILMS

For PZT solid solutions, the dielectric stiffnesses a_1, a_{ij}, a_{ijk} and the electrostrictive constants Q_{ln} have been determined by Haun *et al.* for a set of nine compositions between $x=1$ and 0.[7] The elastic compliances s_{ln}, which are also involved in Eqs. (7)–(13), may be evaluated using the experimental data on the elastic properties of PZT ceramics and PbTiO$_3$ crystals.[27] By averaging the room-temperature compliances measured at constant electric displacement (to comply with the cubic symmetry of paraelectric phase) and interpolating between available experimental points, we obtained the values of s_{ln} given in Table I.

Performing necessary numerical calculations with the aid of Eqs. (7)–(13), we determined equilibrium polarization states of single-domain PZT films with compositions $x = 0.9, 0.8, 0.7, 0.6, 0.5$, and 0.4. Since films were assumed to be sandwiched between two extended electrodes under the short-circuited condition, the electric field **E** in Eq. (7) was set to zero. [The depolarization field in thin films of perovskite ferroelectrics is expected to be negligible due to their finite conductivity (see Ref. 28 and references therein).] The calculations showed that only four different phases may be stable in the studied range of misfit strains S_m and temperatures T. This set of stable phases, which is also characteristic of PbTiO$_3$ epitaxial films,[11] involves the paraelectric phase
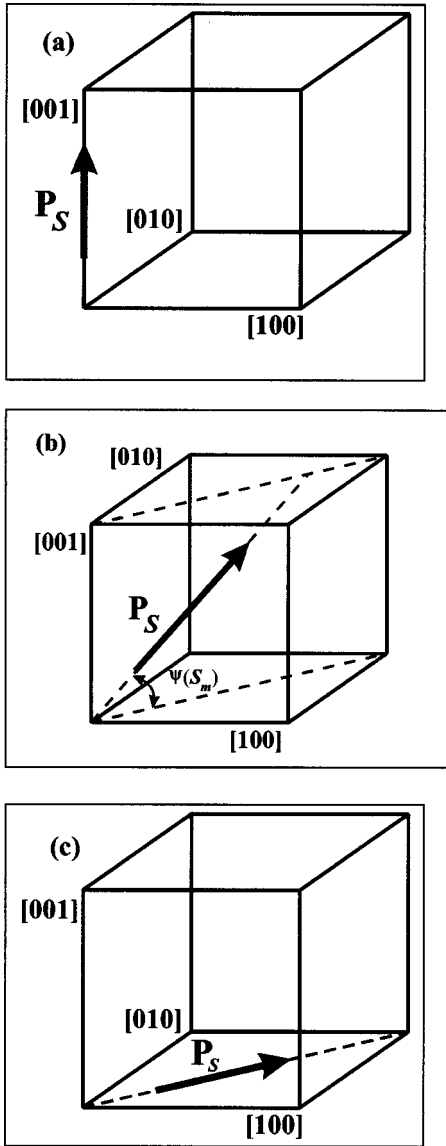
FIG. 1. Orientation of the spontaneous polarization $\mathbf{P}_s$ in stable ferroelectric phases forming in single-domain $Pb(Zr_{1-x}Ti_x)O_3$ thin films grown on (001)-oriented cubic substrates: tetragonal c phase (a), monoclinic r phase (b), and orthorhombic aa phase (c). Polarization orientations are shown relative to the prototypic cubic cell.

$(P_1=P_2=P_3=0)$, the c phase $(P_1=P_2=0, P_3\neq0)$, the aa phase $(P_1=P_2\neq0, P_3=0)$, and the r phase $(P_1=P_2\neq0, P_3\neq0)$ (see Fig. 1). For the investigated compositions x, the stability ranges of these phases in the (S_m,T) plane are shown in Fig. 2.

Discussing the developed (S_m,T) phase diagrams of PZT films, we first note that the temperature T_c of the paraelectric to ferroelectric transformation varies nonmonotonically with the misfit strain S_m. The minimum value of $T_c(S_m)$ coincides with the Curie-Weiss temperature $\theta(x)$ of bulk PZT. This minimum is located at $S_m=0$, where the in-plane lattice parameter $a=b^*$ of a strained epitaxial layer becomes equal to the prototypic cell constant a_0 of a free standing film. The ferroelectric phase transition was found to be of the *second order* for all of the studied compositions x, irrespective of the

misfit strain. For PZT 10/90 and 20/80 ($x=0.9$ and 0.8), the behavior of an epitaxial film differs from that of a bulk material, where the ferroelectric phase transition is of the *first order*.[7] This distinction is caused by the substrate-induced renormalization of the fourth-order polarization terms in the free-energy expansion, which makes the coefficients a_{11}^* and a_{33}^* positive even though the factor a_{11} is negative.

The most characteristic feature of the ferroelectric part of (S_m,T) diagram is the presence of stability range of the *monoclinic r* phase, which is located between the fields of the *tetragonal c* phase and the *orthorhombic aa* phase (Fig. 2). However, the direct transformation of the paraelectric phase into the r phase occurs during cooling only at $S_m=0$ in PZT films with the Ti content x less than about 0.7. At nonzero values of the misfit strain, the paraelectric phase transforms either into the c phase (at $S_m<0$) or into the aa phase (at $S_m>0$) for all compositions x. At $x>0.7$, the stability ranges of these phases have a common boundary at high temperatures, where the first-order aa-phase/c-phase transition should take place.

In the (S_m,T) diagrams of all studied PZT films, the r-phase field is separated from the stability range of the c phase by the first-order transition line. On the contrary, the boundary between the fields of the r and aa phases is defined by the second-order transition. The driving order parameters of these structural transitions are the in-plane polarization components $P_1=P_2$ and the out-of-plane polarization component P_3, respectively. Figure 3 shows how the polarization components P_i vary with the misfit strain S_m at room temperature. It can be seen that the c-phase/r-phase transformation results in the abrupt appearance of finite in-plane polarizations $P_1=P_2$, which is accompanied by a step-like reduction of the out-of-plane polarization P_3. At the r-phase/aa-phase transition, on the other hand, P_3 goes to zero in a continuous manner, whereas the dependence $P_1(S_m)=P_2(S_m)$ only changes its slope.

Inside the "monoclinic gap," the orientation of the polarization vector $\mathbf{P}$ with respect to the substrate normal changes gradually with the misfit strain. At some intermediate value S_m^{rh} of this strain, the out-of-plane and in-plane polarization components become equal to each other so that the r phase appears to be similar to the bulk rhombohedral phase (see Fig. 2). However, the out-of-plane (c) and in-plane (a) lattice parameters of the epitaxial layer generally differ from each other at S_m^{rh}. This feature of thin films follows from Eq. (4), which can be used to calculate the "tetragonality" strain $S_t=c/a-1\cong S_3-S_m$ of the film lattice at $S_m\ll1$. Besides, the in-plane face of the unit cell does not experience shear strains in the r phase due to the mechanical film/substrate interaction ($S_6=0$). The crystal lattice of single-domain films only tilts relative to the substrate normal in the monoclinic gap. This tilt is caused by the appearance of nonzero shear strains S_4 and S_5 in the r phase, which, according to Eqs. (5) and (6), are proportional to the product of the in-plane and out-of-plane polarization components.

As can be seen from Fig. 2, the size and position of the r-phase field in the (S_m,T) plane change with the variation of Ti content x in a PZT film. When x is larger than about
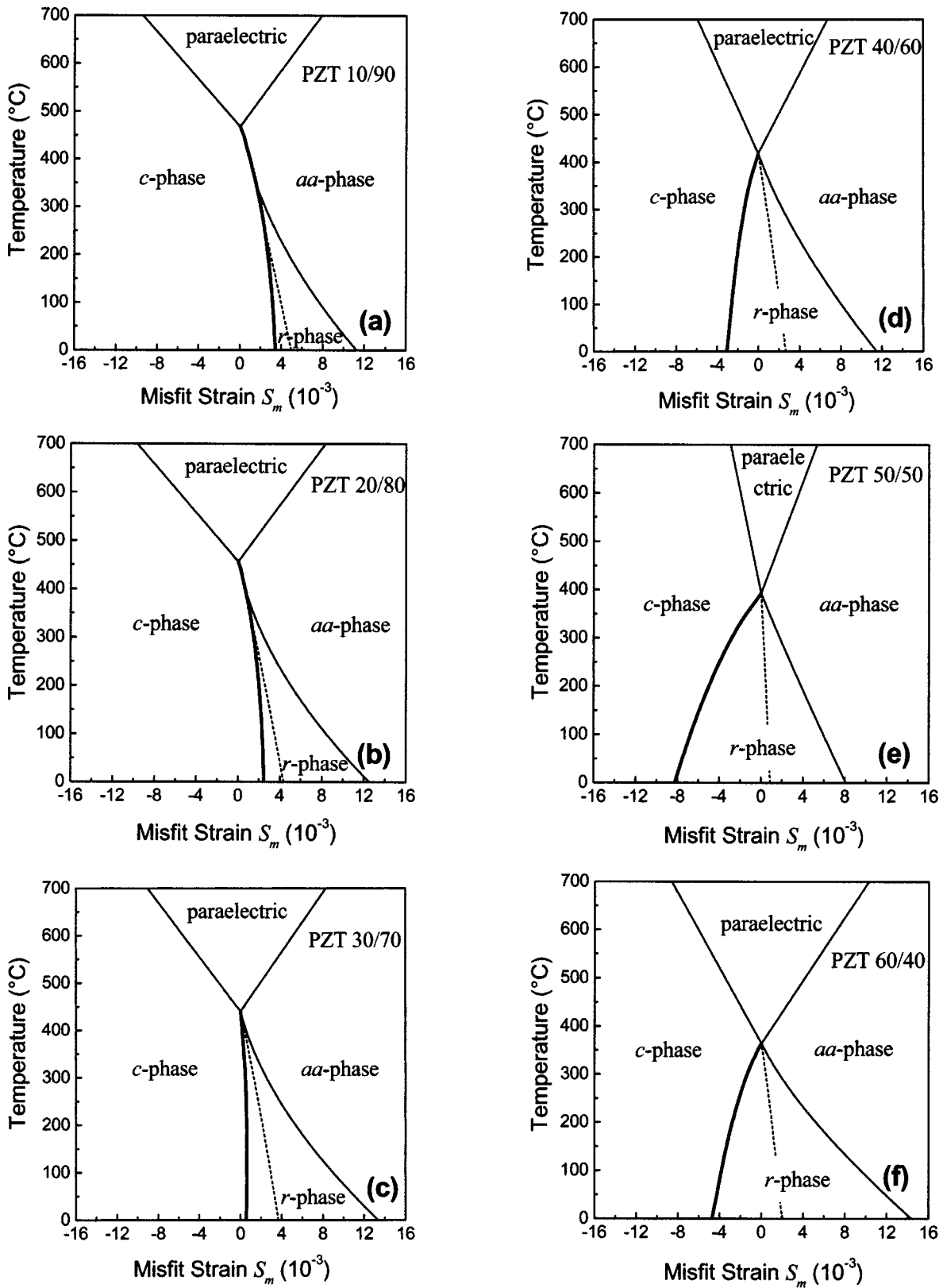
FIG. 2. Phase diagrams of (001)-oriented single-domain $Pb(Zr_{1-x}Ti_x)O_3$ films epitaxially grown on dissimilar cubic substrates. The composition x of the solid solution equals 0.9 (a), 0.8 (b), 0.7 (c), 0.6 (d), 0.5 (e), and 0.4 (f). The second- and first-order phase transitions are shown by thin and thick lines, respectively. The triple or quadruple point at $S_m = 0$ corresponds to the Curie-Weiss temperature $\theta(x)$ of the stress-free bulk material. The dashed line indicates the (S_m, T) conditions, at which the polarization in the r phase becomes oriented along the cube diagonal of the prototypic unit cell ($P_1 = P_2 = P_3$).
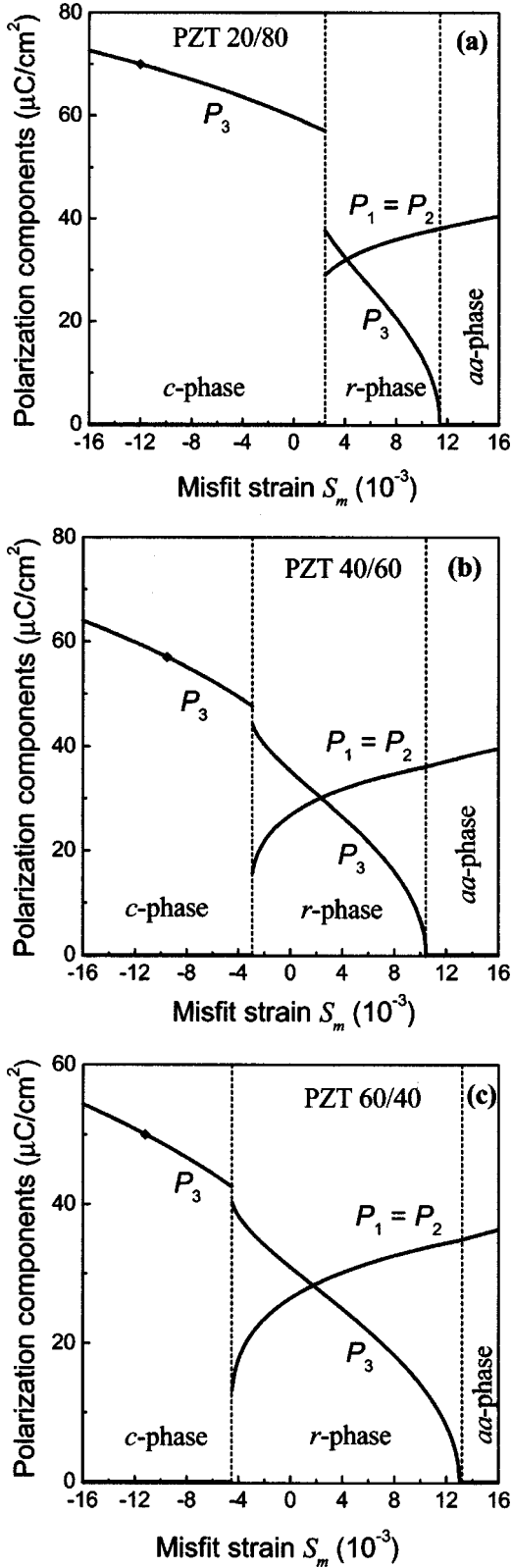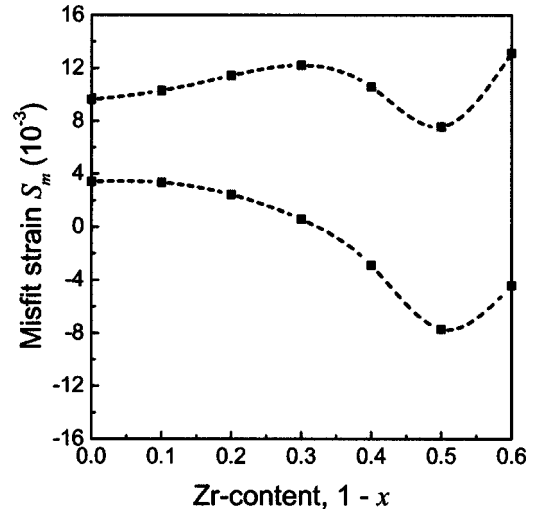
FIG. 4. Stability range of the monoclinic r-phase in epitaxial single-domain PZT films as a function of Zr content. Squares show the calculated positions of two boundaries of the monoclinic gap on the misfit-strain axis at $T = 25\,^\circ$C. The dashed line is a guide for the eye.

0.7, the monoclinic gap does not exist at high temperatures close to the Curie-Weiss temperature $\theta(x)$ of a bulk material. For these compositions, two triple points are present in the phase diagram in similarity with the case of PbTiO$_3$.[11] At $x \leq 0.7$, the stability range of the r phase extends up to θ so that the triple points merge into a quadruple one.

The effect of composition on the location of the monoclinic gap on the misfit-strain axis at room temperature is shown in Fig. 4. With the increase of Zr content, the left boundary of this gap shifts from positive to negative misfit strains. The maximum shift towards negative values of S_m occurs near $x = 0.5$, i.e., close to the MPB of bulk PZT. The position of the right boundary varies nonmonotonically with the composition, changing the trend at $x \approx 0.5$ and 0.7. Remarkably, the stability range of the r phase *widens* with the increase of Zr content in a PZT film (see Fig. 4).

IV. DIELECTRIC AND PIEZOELECTRIC RESPONSES OF SINGLE-DOMAIN PZT FILMS

Consider now the responses of epitaxial PZT films to the application of a uniform electric field. The dependence of the polarization components P_i in a single-domain film on the field intensity $\mathbf{E}$ can be found using Eq. (7) and the condition $\partial \widetilde{G} / \partial P_i = 0$. The reversible field-induced variations of P_i determine the dielectric susceptibilities $\eta_{ij} = \partial P_i / \partial E_j$ of a ferroelectric film. Owing to the electrostriction, these variations also give rise to changes of the lattice strains S_n in an epitaxial layer. The resulting converse piezoelectric effect may be described by the coefficients $d_{in} = \partial S_n / \partial E_i$.

By differentiating the modified thermodynamic potential $\widetilde{G}$, we can derive explicit expressions for the reciprocal dielectric susceptibilities $\chi_{ij} = \partial^2 \widetilde{G} / \partial P_i \partial P_j$. The matrix inversion then enables us to find the dielectric susceptibilities

FIG. 3. Misfit-strain dependence of the polarization components $P_1 = P_2$ and P_3 in single-domain epitaxial Pb(Zr$_{1-x}$Ti$_x$)O$_3$ films at the room temperature $T = 25\,^\circ$C. The Ti content x equals 0.8 (a), 0.6 (b), and 0.4 (c). The diamond symbols show the theoretical polarizations of bulk PZT single-crystals, which were calculated in Ref. 7.

$\eta_{ij} = \chi_{ij}^{-1}$ and permittivities $\varepsilon_{ij} = \varepsilon_0 + \eta_{ij}$ of a thin film. The calculated dielectric constants ε_{ij} depend on the polarization $\mathbf{P}(\mathbf{E})$ existing in a ferroelectric film. Restricting our analysis to the small-signal dielectric responses $\varepsilon_{ij}(\mathbf{E} \to 0)$, we can find the film permittivities ε_{ij} using the equilibrium polarization components $P_i(\mathbf{E} = 0)$ determined in Sec. III. It should be noted that the stability ranges of the c, r, and aa phases in the (S_m, T) plane must be taken into account in the calculations of the film dielectric constants and their misfit-strain and temperature dependences.

The most important dielectric characteristic of a ferroelectric thin film is the out-of-plane permittivity ε_{33}, which is measured in a conventional plate-capacitor setup, where the applied electric field $\mathbf{E}$ is orthogonal to the film surfaces. We calculated numerically the dependence of this permittivity on the misfit strain S_m at room temperature. Figure 5 shows the theoretical results obtained for PZT films with three representative compositions. It can be seen that the film permittivity varies nonmonotonically with the misfit strain existing in the epitaxial system. The strain-induced structural transformations between different polarization states manifest themselves in the dielectric anomalies. The first-order c-phase/r-phase transition is accompanied by a step-like increase of the out-of-plane permittivity ε_{33}. A small peak of ε_{33}, which appears at misfit strains slightly exceeding the threshold value in PZT films with a large Zr content [see Figs. 3(b) and 3(c)], may be explained by the relation $\eta_{33} = (\chi_{11} + \chi_{12})/[\chi_{33}(\chi_{11} + \chi_{12}) - 2\chi_{13}^2]$. This relation determines the out-of-plane response of the r phase, and shows that η_{33} increases due to the presence of a nonzero reciprocal susceptibility χ_{13} in this phase. In turn, at the second-order r-phase/aa-phase transition the theoretical permittivity ε_{33} of PZT films diverges so that an anomalous increase of the out-of-plane dielectric response may be expected near the corresponding critical misfit strain.

Consider next the small-signal piezoelectric responses of epitaxial PZT films, which can measured in a conventional plate-capacitor setup. The coefficients d_{in}, which determine the converse piezoelectric effect, are calculated as $d_{in} = \partial S_n / \partial E_i = b_{kn} \eta_{ki}$, where $b_{kn} = \partial S_n / \partial P_k$. Since the measuring electric field $\mathbf{E}$ is applied along the x_3 axis orthogonal to the film surfaces, we restrict our analysis to the coefficients d_{3n}. However, the in-plane sizes and shape of the film are governed by a much thicker substrate so that the piezoelectric responses d_{31}, d_{32}, and d_{36} are equal to zero in our approximation. The remaining coefficients d_{33}, d_{34}, and d_{35} characterize the field-induced change of the film thickness and a tilt of the ferroelectric overlayer relative to the substrate normal. To find these coefficients, we first calculated the relevant piezoelectric constants $b_{kn} = \partial S_n / \partial P_k$ by differentiating Eqs. (4)–(6) for the film strains S_3, S_4, and S_5 and using the equilibrium polarization components $P_i(\mathbf{E} = 0)$ reported in Sec. III. The coefficients d_{33}, d_{34}, and d_{35} were then evaluated numerically as functions of the misfit strain S_m and temperature T with the account of the known dielectric susceptibilities η_{k3} of PZT films.
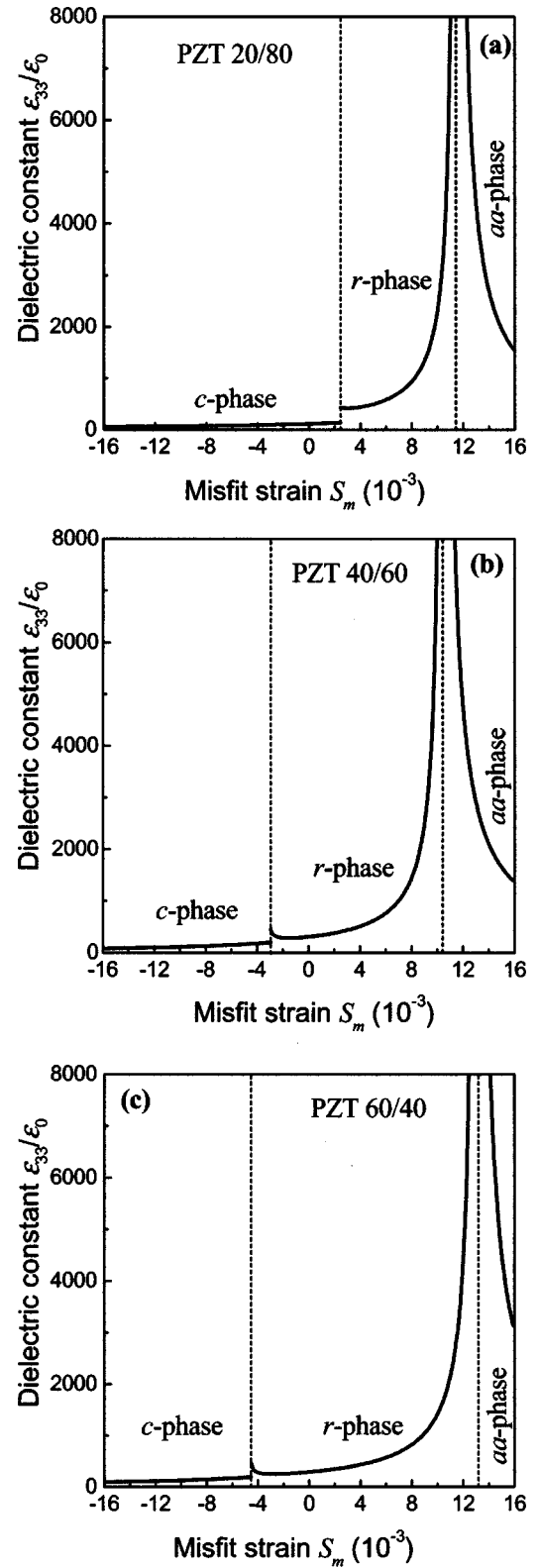

FIG. 5. Out-of-plane dielectric response ε_{33} of epitaxial single-domain Pb(Zr$_{1-x}$Ti$_x$)O$_3$ films calculated as a function of the misfit strain at $T = 25\,^{\circ}$C. The film composition x equals 0.8 (a), 0.6 (b), and 0.4 (c).
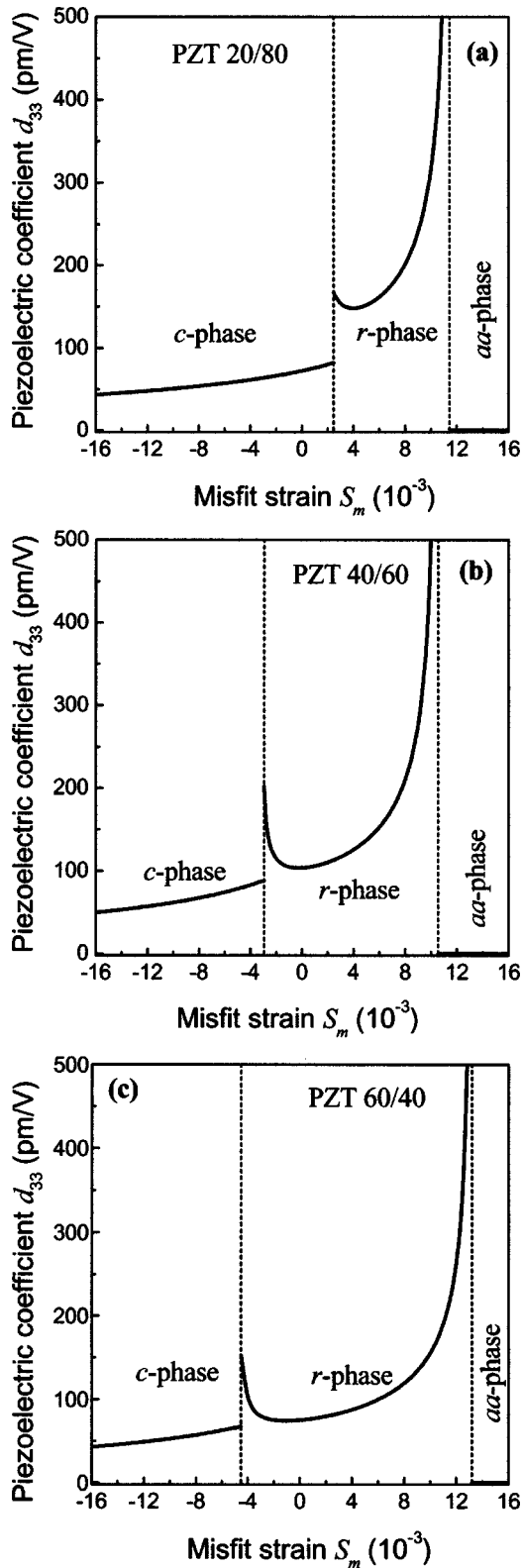
FIG. 6. Piezoelectric coefficient d_{33} of epitaxial single-domain Pb(Zr$_{1-x}$Ti$_x$)O$_3$ films as a function of the misfit strain at T = 25 °C. The film composition x equals 0.8 (a), 0.6 (b), and 0.4 (c).

The variation of the longitudinal piezoelectric coefficient d_{33} with the misfit strain S_m at room temperature is shown in Fig. 6 for PZT films with three representative compositions. In the tetragonal c phase, the piezoelectric response d_{33} increases as the misfit strain tends to a critical value, at which this phase is replaced by the monoclinic r phase in the (S_m,T) diagram. The jump of d_{33} at this structural transformation is followed by a nonmonotonic variation of the piezoelectric response in films containing the r phase. This behavior is partly caused by specific dependence of the film out-of-plane permittivity ε_{33} on the misfit-strain (see Fig. 5). In particular, the divergence of ε_{33} at the r-phase/aa-phase transition leads to abnormal increase of the piezoelectric coefficient d_{33} in close vicinity to the critical misfit strain. Finally, the piezoelectric response vanishes at large positive S_m due to the absence of the out-of-plane polarization P_3 in the orthorhombic aa phase (see Fig. 6).

V. CONCLUDING REMARKS

The nonlinear thermodynamic theory shows that the equilibrium polarization states of single-domain PZT films are sensitive to both the misfit strain S_m in an epitaxial system and the composition of the solid solution. The most interesting theoretical prediction is concerned with the formation of the strain-induced *monoclinic* phase in PZT films. In this r phase, the polarization **P** is oriented in the $[uuv]$ crystallographic direction so that it is confined to a mirror plane (see Fig. 1). Accordingly, the r phase is similar to the monoclinic phase (space group Bm), which was observed in the bulk PZT 52/48 ceramic.[5,6] However, the existence of the "monoclinic field" in the (S_m,T) phase diagrams of PZT films is not restricted to compositions close to the MPB (Fig. 2). At room temperature, the monoclinic gap on the misfit-strain axis is present for all of the studied compositions. The bulk MPB manifests itself only in the position of the center of this gap, which becomes close to $S_m=0$ at $x \approx 0.5$ (see Fig. 4).

The predicted formation of the r phase in strained PZT thin films is supported by the recent experimental observations of Kelman *et al.*[29] These authors investigated the structural properties of (001)-oriented polycrystalline PZT 35/65 films deposited onto Si wafers at $T_g=570$ °C. High-resolution x-ray diffraction showed that in films thinner than 150 nm, which consist of single-domain columnar grains, the crystal structure becomes similar to a rhombohedral one (instead of tetragonal structure observed in bulk PZT 35/65 ceramics and in thicker films with polydomain grains). This phase transformation may be successfully explained by the two-dimensional straining of a thin PZT film grown on the Si substrate. Indeed, the calculation gives the value of $S_m \approx 1 \times 10^{-3}$ for the misfit strain in the discussed film/substrate system.[30] As can be seen from Fig. 4, this value falls into the monoclinic gap predicted for epitaxial PZT 35/65 films. Moreover, the tetragonality strain of PZT 35/65 film at $S_m \approx 1 \times 10^{-3}$ is estimated to be of the order of 5×10^{-3}, which is much smaller than the tetragonality strain $S_t \approx 4 \times 10^{-2}$ of

bulk PZT 35/65.[7] The small lattice tetragonality of the monoclinic r phase, which is expected to form in single-domain PZT 35/65 films grown on Si, makes it similar to a rhombohedral phase (with respect to the x-ray-diffraction data). This feature explains why Kelman *et al.*[29] regarded the crystal structure of their thinnest PZT 35/65 films as a rhombohedral one.

Consider now the effect of composition on the remanent polarization in epitaxial PZT films. Foster *et al.* reported the systematic compositional variation of the ferroelectric properties of (001)-oriented single-crystalline PZT films grown on SrRuO$_3$ buffered SrTiO$_3$ crystals.[19] It was found that the remanent polarization measured in a plate-capacitor setup varies nonmonotonically with Zr content and has a minimum near the bulk MPB. To compare theoretical predictions with this experimental result, we calculated the out-of-plane polarization P_3 of a single-domain PZT film as a function of Zr content, assuming that the misfit strain in the PZT/SrTiO$_3$ epitaxial system is equal to $S_m = -3 \times 10^{-3}$, irrespective of the composition.[33] The theoretical dependence $P_3(x)$ is presented in Fig. 7, which shows that the film out-of-plane polarization becomes minimum near $x = 0.5$, where it has a value of about 35 μC/cm^2. These results of thermodynamic calculations are in good agreement with the observations of Foster *et al.*, who found the minimum remanent polarization of 34 μC/cm^2 in submicron-thick PZT 56/44 films.[19]

Finally, we would like to emphasize that, according to the nonlinear thermodynamic theory, the out-of-plane polarization P_3 of an epitaxial PZT film may exceed the bulk spontaneous polarization P_s. Such polarization superiority is characteristic of PZT films grown on "compressive" substrates, which create a large negative misfit strain in the epitaxial system ($S_m < -12 \times 10^{-3}$; see Fig. 3). This condition could be fulfilled only in the film/substrate systems with $b(T_g) < a_0(T_g)$, provided the film is sufficiently thin to avoid complete relaxation of $S_m(T_g)$ via the generation of misfit dislocations at the growth temperature T_g. The above theoretical prediction seems to be confirmed by our recent
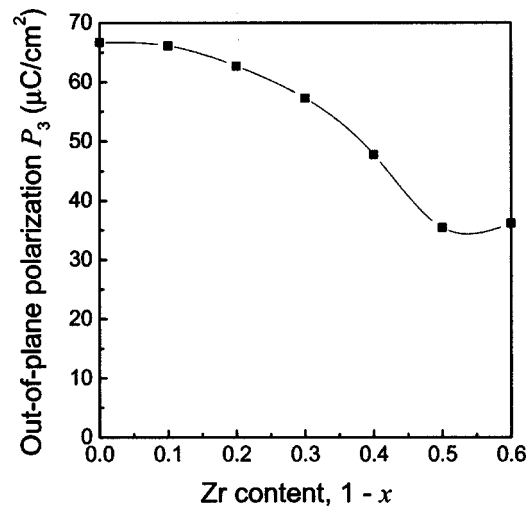

FIG. 7. Out-of-plane polarization P_3 of Pb(Zr$_{1-x}$Ti$_x$)O$_3$ films at $T = 25\,°$C as a function of Zr content. The misfit strain S_m in the epitaxial system is taken to be equal to -3×10^{-3}, which corresponds to thick PZT films grown on SrTiO$_3$. Squares show the calculated values, and the line is a guide for the eye.

experimental study of the ferroelectric properties of very thin (thickness ~ 10–10^2 nm) epitaxial PZT 52/48 films deposited on SrRuO$_3$-covered SrTiO$_3$ crystals.[24] The measurements of ferroelectric hysteresis loops showed that the remanent polarization in these films is about 52.5 μC/cm^2, which is larger than the spontaneous polarization $P_s = 50\,\mu$C/cm^2 expected in the bulk PZT 52/48 single crystal.[7]

*Permanent address: A. F. Ioffe Physico-Technical Institute, Russian Academy of Sciences, 194021 St. Petersburg, Russia. Electronic address: pertsev@domain.ioffe.rssi.ru

[1] K. Uchino, *Piezoelectric Actuators and Ultrasonic Motors* (Kluwer, Boston, 1996).

[2] O. Auciello, J. F. Scott, and R. Ramesh, Phys. Today **51** (7), 22 (1998).

[3] N. Setter and R. Waser, Acta Mater. **48**, 151 (2000).

[4] B. Jaffe, W. R. Cook, and H. Jaffe, *Piezoelectric Ceramics* (Academic, London, 1971).

[5] B. Noheda, D. E. Cox, G. Shirane, J. A. Gonzalo, L. E. Cross, and S.-E. Park, Appl. Phys. Lett. **74**, 2059 (1999).

[6] B. Noheda, J. A. Gonzalo, L. E. Cross, R. Guo, S.-E. Park, D. E. Cox, and G. Shirane, Phys. Rev. B **61**, 8687 (2000).

[7] M. J. Haun, E. Furman, S. J. Jang, and L. E. Cross, Ferroelectrics **99**, 13 (1989), Secs. I–V.

[8] D. Vanderbilt and M. H. Cohen, Phys. Rev. B **63**, 094108 (2001).

[9] L. Bellaiche, A. Garcia, and D. Vanderbilt, Phys. Rev. Lett. **84**, 5427 (2000).

[10] S. H. Oh and H. M. Jang, Appl. Phys. Lett. **72**, 1457 (1998); Phys. Rev. B **62**, 14 757 (2000); **63**, 132101 (2001).

[11] N. A. Pertsev, A. G. Zembilgotov, and A. K. Tagantsev, Phys. Rev. Lett. **80**, 1988 (1998); Ferroelectrics **223**, 79 (1999).

[12] N. A. Pertsev, A. K. Tagantsev, and N. Setter, Phys. Rev. B **61**, R825 (2000); **65**, 219901 (2002).

[13] N. A. Pertsev and V. G. Koukhar, Phys. Rev. Lett. **84**, 3722 (2000).

[14] V. G. Koukhar, N. A. Pertsev, and R. Waser, Phys. Rev. B **64**, 214103 (2001).

[15] J. Lee, A. Safari, and R. L. Pfeffer, Appl. Phys. Lett. **61**, 1643 (1992).

[16] M. de Keijser, J. F. M. Cillessen, R. B. F. Janssen, A. E. M. De Veirman, and D. M. de Leeuw, J. Appl. Phys. **79**, 393 (1996).

[17] J.-M. Triscone, L. Frauchiger, M. Decroux, L. Miéville, Ø. Fisher, C. Beeli, P. Stadelmann, and G.-A. Racine, J. Appl. Phys. **79**, 4298 (1996).

[18] T. Yu, Y.-F. Chen, Z.-G. Liu, S.-B. Xiong, L. Sun, X.-Y. Chen, L.-J. Shi, and N.-B. Ming, Appl. Phys. Lett. **69**, 2092 (1996).

[19] C. M. Foster, G.-R. Bai, R. Csencsits, J. Vetrone, R. Jammy, L. A. Wills, E. Carr, and J. Amano, J. Appl. Phys. **81**, 2349 (1997).

[20] T. Tybell, C. H. Ahn, and J.-M. Triscone, Appl. Phys. Lett. **75**, 856 (1999).

[21] V. Nagarajan, I. G. Jenkins, S. P. Alpay, H. Li, S. Aggarval, L. Salamanca-Riba, A. L. Roytburd, and R. Ramesh, J. Appl. Phys. **86**, 595 (1999).

[22] O. Kuffer, I. Maggio-Aprile, J.-M. Triscone, Ø Fisher, and Ch. Renner, Appl. Phys. Lett. **77**, 1701 (2000).

[23] K. Nagashima, M. Aratani, and H. Funakubo, J. Appl. Phys. **89**, 4517 (2001).

[24] J. Rodríguez Contreras, J. Schubert, U. Poppe, O. Trithaveesak, K. Szot, Ch. Buchal, H. Kohlstedt, and R. Waser, in *Ferroelectric Thin Films X*, edited by S. R. Gilbert, Y. Miyasaka, D. Wouters, S. Trolier-McKinstry, and S. K. Streiffer, MRS Symposia Proceedings No. 688 (Materials Research Society, Pittsburgh, 2002), p. C8.10.

[25] F. Jona and G. Shirane, *Ferroelectric Crystals* (MacMillan, New York, 1962).

[26] J. S. Speck and W. Pompe, J. Appl. Phys. **76**, 466 (1994).

[27] *Crystal and Solid State Physics*, edited by K.-H Hellwege and A. M. Hellwege, Landolt-Börnstein, New Series, Group III, Vol. 1 (Springer-Verlag, Berlin, 1966).

[28] H. Kohlstedt, N. A. Pertsev, and R. Waser, in *Ferroelectric Thin Films X* (Ref. 24), p. 161.

[29] M. B. Kelman, L. F. Schloss, P. C. McIntyre, B. C. Hendrix, S. M. Bilodeau, and J. F. Roeder, Appl. Phys. Lett. **80**, 1258 (2002).

[30] For the considered relatively thick PZT films, the misfit strain $S_m = (b^* - a_0)/a_0$ is expected to be fully relaxed ($b^* = a_0$) at the deposition temperature T_g. The increase of S_m during the cooling from T_g to the room temperature can be evaluated using the measured nonlinear thermal expansion of Si (see Ref. 31) and the thermal expansion coefficient of PZT 35/65 (about 6.2 $\times 10^{-6}$ according to the data given in Ref. 32).

[31] *Physics of Group IV Elements and III-V Compounds*, edited by O. Madelung, Landolt-Börnstein, New Series, Group III, Vol. 17, pt. a (Springer-Verlag, Berlin, 1982), p. 61.

[32] Y. S. Touloukian, R. K. Kirby, R. E. Taylor, and T. Y. R. Lee, *Thermal Expansion, Nonmetallic Solids*, Thermophysical Properties of Matter, Vol. 13 (Plenum, New York, 1997).

[33] This value of S_m corresponds to submicron-thick PZT films deposited on $SrTiO_3$ at $T_g = 600\,°C$ (as in Ref. 19). It was calculated by assuming $S_m(T_g) = 0$ and using the thermal expansion coefficients of $SrTiO_3$ (11×10^{-6} K^{-1}) and PZT ($\approx 6 \times 10^{-6}$ K^{-1}), which were taken from Ref. 32.